Regular Article

blood

LYMPHOID NEOPLASIA

FZR1 loss increases sensitivity to DNA damage and consequently promotes murine and human B-cell acute leukemia

Jo Ishizawa,[1-3] Eiji Sugihara,[1] Shinji Kuninaka,[1] Kaoru Mogushi,[4] Kensuke Kojima,[3,5] Christopher B. Benton,[3] Ran Zhao,[3] Dhruv Chachad,[3] Norisato Hashimoto,[1,2] Rodrigo O. Jacamo,[3] Yihua Qiu,[3] Suk Young Yoo,[6] Shinichiro Okamoto,[2] Michael Andreeff,[3] Steven M. Kornblau,[3] and Hideyuki Saya[1]

[1]Division of Gene Regulation, Institute for Advanced Medical Research, and [2]Division of Hematology, Department of Medicine, Keio University School of Medicine, Tokyo, Japan; [3]Department of Leukemia, The University of Texas MD Anderson Cancer Center, Houston, TX; [4]Intractable Disease Research Center, Graduate School of Medicine, Juntendo University, Tokyo, Japan; [5]Hematology, Respiratory Medicine, and Oncology, Department of Medicine, Saga University, Saga, Japan; and [6]Department of Bioinformatics and Computational Biology, The University of Texas MD Anderson Cancer Center, Houston, TX

Key Points

- FZR1 loss causes increased sensitivity of B-ALL cells to oncogene- or chemotherapy-induced DNA damage.
- Prolonged loss of FZR1 contributes to the development of treatment-resistant clones in mouse and human B-ALL.

FZR1 (fizzy-related protein homolog; also known as CDH1 [cell division cycle 20 related 1]) functions in the cell cycle as a specific activator of anaphase-promoting complex or cyclosome ubiquitin ligase, regulating late mitosis, G_1 phase, and activation of the G_2-M checkpoint. FZR1 has been implicated as both a tumor suppressor and oncoprotein, and its precise contribution to carcinogenesis remains unclear. Here, we examined the role of FZR1 in tumorigenesis and cancer therapy by analyzing tumor models and patient specimens. In an *Fzr1* gene-trap mouse model of B-cell acute lymphoblastic leukemia (B-ALL), mice with *Fzr1*-deficient B-ALL survived longer than those with *Fzr1*-intact disease, and sensitivity of *Fzr1*-deficient B-ALL cells to DNA damage appeared increased. Consistently, conditional knockdown of FZR1 sensitized human B-ALL cell lines to DNA damage–induced cell death. Moreover, multivariate analyses of reverse-phase protein array of B-ALL specimens from newly diagnosed B-ALL patients determined that a low FZR1 protein expression level was an independent predictor of a longer remission duration. The clinical benefit of a low FZR1 expression level at diagnosis was no longer apparent in patients with relapsed B-ALL. Consistent with this result, secondary and tertiary mouse recipients of *Fzr1*-deficient B-ALL cells developed more progressive and radiation-resistant disease than those receiving *Fzr1*-intact B-ALL cells, indicating that prolonged inactivation of *Fzr1* promotes the development of resistant clones. Our results suggest that reduction of FZR1 increases therapeutic sensitivity of B-ALL and that transient rather than tonic inhibition of FZR1 may be a therapeutic strategy. (*Blood*. 2017;129(14):1958-1968)

Introduction

FZR1 (fizzy-related protein homolog; also known as CDH1 [cell division cycle 20 related 1]) specifically activates the anaphase-promoting complex or cyclosome (APC/C), a ubiquitin ligase that plays a key regulatory role between late mitotic and G_1 phases of the cell cycle. During late mitosis, FZR1 replaces CDC20, which is the activator of APC/C during early mitosis. This switch results in the ubiquitination of various cell cycle modulators, including PLK1, SKP2, and GMNN.[1-5] FZR1 also contributes to the regulation of postmitotic[6] and quiescent (G_0)[7,8] states.

In addition to functioning in cell cycle regulation,[9,10] evidence suggests that FZR1 plays an important role in the DNA damage response (DDR). We previously demonstrated FZR1 is essential for DNA damage–induced G_2 arrest in chicken B-cell lymphoma (DT40) cells, with loss of FZR1 resulting in an aberrant G_2 checkpoint and sensitization of the cells to radiation.[11] The induction of DNA double-strand breaks (DSBs) by radiation was also shown to trigger the nucleoplasmic localization of the phosphatase CDC14B, resulting in the dephosphorylation and activation of FZR1, G_2 arrest, and DNA repair.[12] We previously generated a tissue-specific conditional *Fzr1* gene-trap (GT) mouse[13] to overcome the embryonic lethality of homozygous *Fzr1* knockout[10] or GT.[14] Our analysis of these animals revealed that the radiation-induced G_2-M checkpoint is defective in *Fzr1*-deficient nonmalignant bone marrow (BM) cells, resulting in increased probability of mitotic catastrophe during radiation-induced stress.[13]

The expression of *FZR1* has been found to be reduced or lost in various human cancers,[12,15] suggesting *FZR1* may function as a tumor suppressor. *Fzr1* heterozygous GT mice were also shown to be more likely to develop epithelial tumors than wild-type (WT) mice,[10] indicating that *Fzr1* is a haploinsufficient tumor suppressor. On the other hand, observations that loss of *Fzr1* induces cell death in neural and hematopoietic progenitor cells[6,9,11,13,16] suggest that FZR1 may be essential for malignant cells to survive. The precise role of FZR1 in tumorigenesis has remained ill defined.

Submitted 18 July 2016; accepted 25 January 2017. Prepublished online as *Blood* First Edition paper, 31 January 2017; DOI 10.1182/blood-2016-07-726216.

The online version of this article contains a data supplement.

The publication costs of this article were defrayed in part by page charge payment. Therefore, and solely to indicate this fact, this article is hereby marked "advertisement" in accordance with 18 USC section 1734.

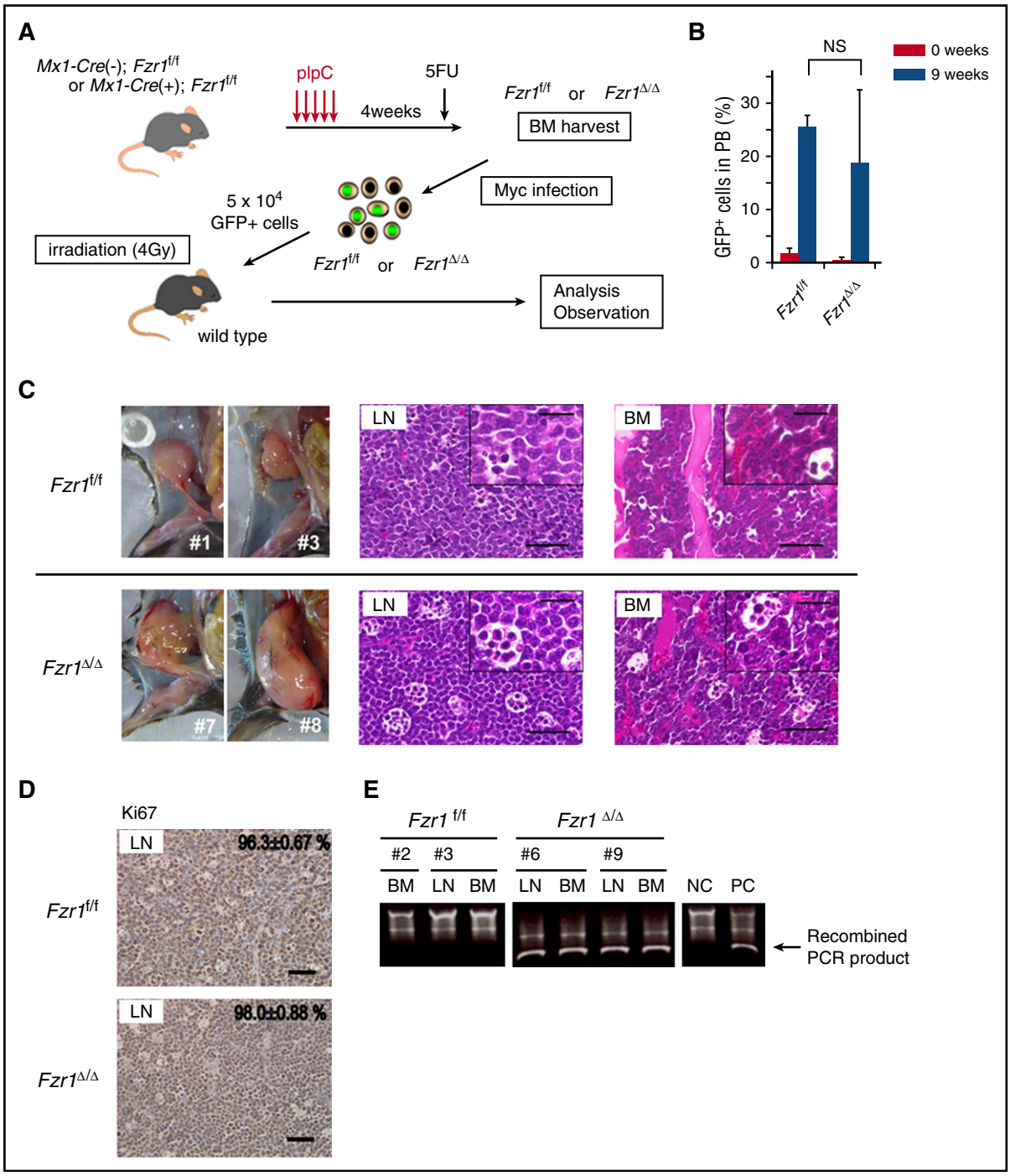

Figure 1. *Fzr1*-intact and *Fzr1*-deficient B-ALL share similar pathological characteristics. (A) Experimental design for retrovirus-mediated introduction of *Mycn* into *Fzr1*-intact ($Fzr1^{f/f}$) or *Fzr1*-deficient ($Fzr1^{\Delta/\Delta}$) BM-MNCs and transplantation of the infected cells into WT recipient mice (see Materials and methods for experimental details). 5FU, 5-fluorouracil. (B) Flow cytometry–based determination of the proportion of GFP^+ cells in the PB of recipient mice immediately and 9 weeks after transplantation of *Mycn*-overexpressing *Fzr1*-intact or *Fzr1*-deficient BM-MNCs. The data are presented as mean ± standard deviation (SD) (n = 3 mice per group). NS, not significant; $P = .44$. (C) Gross appearance of enlarged lymph nodes (left) as well as hematoxylin and eosin staining of affected LNs (middle) and BM (right) in mice given *Fzr1*-intact (top) or *Fzr1*-deficient (bottom) cells when they became moribund. Insets show higher-magnification views. Scale bars, 50 μm (low power) or 20 μm (high power). (D) Immunohistochemical staining of Ki67 in affected lymph nodes as in panel C. The percentages of $Ki67^+$ cells are shown as mean ± SD determined for 3 mice of each group. Scale bars, 50 μm. (E) Representative PCR-based genotyping of sorted GFP^+ cells from affected lymph nodes or BM of individual recipient mice. NC, negative control consisting of genomic DNA from BM cells of *Mx1-Cre*(−);$Fzr1^{f/f}$ mice; PC, positive control, consisting of genomic DNA from BM cells of *Mx1-Cre*(+);$Fzr1^{f/f}$ mice after pIpC injection.

To determine whether FZR1 promotes or inhibits tumorigenesis in vivo, we have combined tissue-specific conditional *Fzr1* GT mice[13] with a MYC-induced B-cell acute lymphoblastic leukemia (B-ALL) model[17] and compared phenotypes of *Fzr1*-intact vs *Fzr1*-deficient B-ALL mice. We also analyzed FZR1 expression in primary B-ALL cells derived from 224 adult patients with the use of a reverse-phase protein array (RPPA). Our results suggest that loss of FZR1 initially renders B-ALL cells less

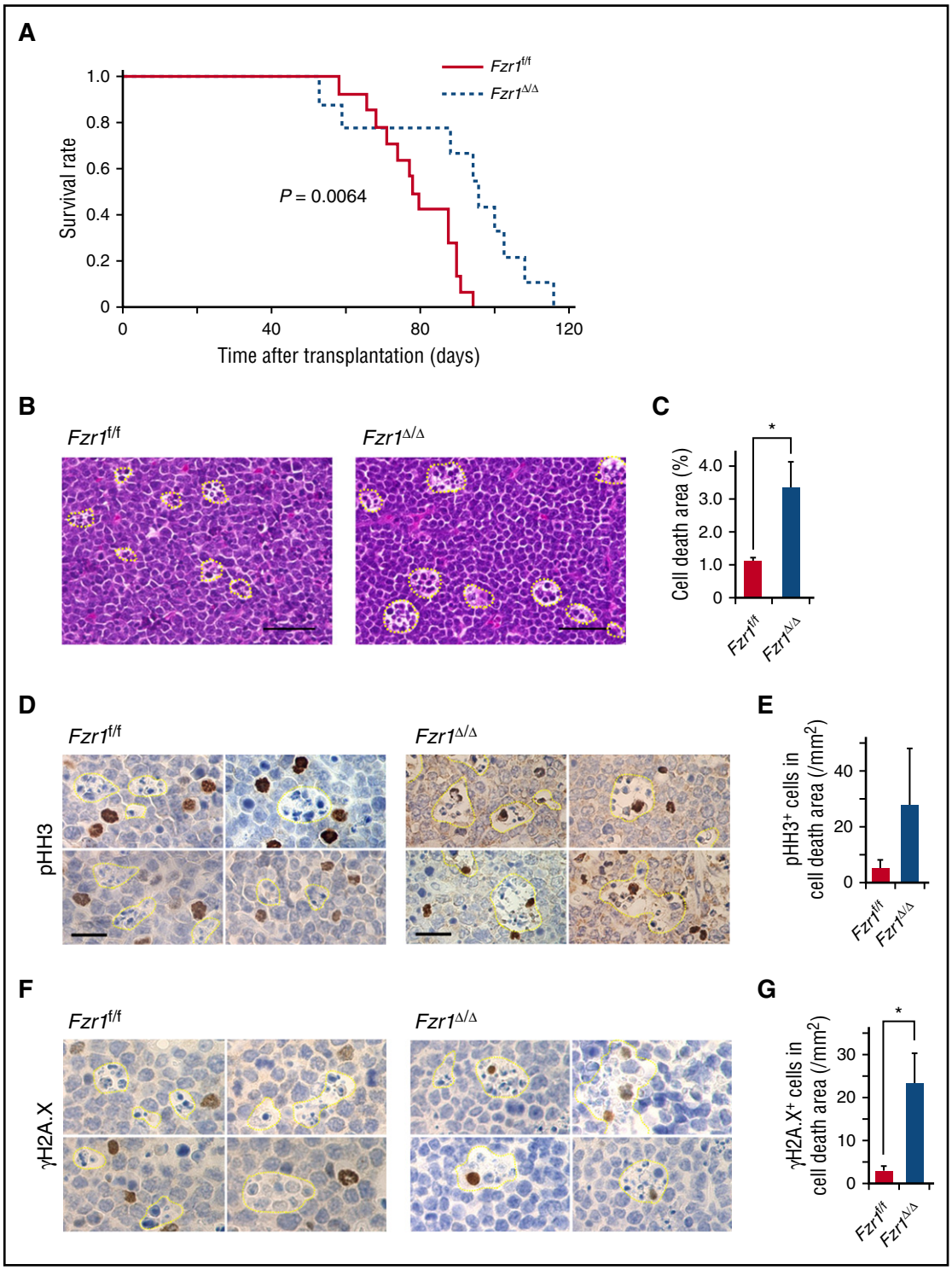

Figure 2. Longer survival in mice with *Fzr1*-deficient B-ALL than in those with *Fzr1*-intact B-ALL is associated with increased B-ALL cell fragility induced by DNA DSBs. (A) Survival curves for mice with B-ALL originating from *Fzr1*-intact (n = 14 mice) or *Fzr1*-deficient (n = 9 mice) BM cells. The *P* value was determined with the log-rank test. (B) Areas of cell death (outlined with yellow dotted lines) in hematoxylin and eosin–stained sections of B-ALL–affected lymph nodes from moribund recipient mice. Scale bars, 50 μm. (C) Proportion of lymph nodes occupied by areas of cell death as determined for sections in panel B. The data are presented as the mean ± SD (n = 3 mice per group). **P* = .049. (D and F) Immunohistochemical staining for pHH3 (D) and γH2A.X (F) in affected lymph nodes from mice with *Fzr1*-intact or *Fzr1*-deficient B-ALL. Scale bars, 20 μm. (E and G) Density of cells positive for pHH3 (E) or γH2A.X (G) in areas of cell death as determined for sections similar to those in panels D and F, respectively. The data are presented as mean ± SD (n = 3 mice per group). *P* = .191 for pHH3; **P* = .0077 for γH2A.X.

robust because of increased sensitivity to DNA damage; however, over time, FZR1 loss leads to the generation of resistant clones that give rise to progressive disease. We propose that FZR1 expression predicts chemosensitivity of B-ALL cells and that transient inhibition of FZR1 is a potential therapeutic strategy for B-ALL.

Table 1. The top 20 enriched gene signatures determined by GSEA for GFP$^+$ BM-MNCs isolated from mice given *Fzr1*-deficient B-ALL cells relative to those from mice given *Fzr1*-intact B-ALL cells

Gene set (reactome)	NES	*P*	FDR
Toll-like receptor 4 cascade	2.08	<.001	0.006
MYD88 cascade	1.89	.002	0.050
Activated TLR4 signaling	1.82	<.001	0.083
Metal ion SLC transporters	1.82	.006	0.063
G2-M checkpoints	**1.72**	**.002**	**0.163**
Late phase of HIV life cycle	1.71	<.001	0.151
Toll-like receptor 9 cascade	1.71	.006	0.133
Vpr-mediated nuclear import of PICs	1.68	<.001	0.145
snRNP assembly	1.68	.006	0.133
Transport of ribonucleoproteins into the host nucleus	1.64	.017	0.186
Nuclear import of rev protein	1.62	.024	0.190
Transport of mature mRNA derived from an intron containing transcript	1.61	.006	0.198
Rev mediated nuclear export of HIV1 RNA	1.61	.017	0.183
NEP/NS2 interacts with the cellular export machinery	1.61	.028	0.172
Activation of ATR in response to replication stress	**1.60**	**.028**	**0.167**
Transcription of the HIV genome	1.60	.004	0.160
Mitotic prometaphase	**1.59**	**.004**	**0.163**
Glycogen breakdown glycogenolysis	1.58	.025	0.177
Metabolism of RNA	1.54	.015	0.227
HIV life cycle	1.52	.011	0.244

Bold type indicates 3 gene sets related to mitosis or DDR.
FDR, false-discovery rate; NES, normalized enrichment score.

Materials and methods

Mice

All mouse experiments were performed under approval of the Institutional Animal Care and Use Committee of Keio University School of Medicine and in accordance with the National Institutes of Health's *Guide for the Care and Use of Laboratory Animals*. C57BL/6 mice (7 to 8 weeks of age) were obtained from Sankyo Labo Service (Tokyo, Japan). *Fzr1*$^{+/GT}$ (C57BL/6 background), *Fzr1*$^{GT[f\text{-}cDNA]/GT[f\text{-}cDNA]}$ (*Fzr1*$^{f/f}$), and *Mx1-Cre* transgenic mice were obtained from TransGenic (Kumamoto, Japan) as previously described.[13,14,18] Supplemental Materials and methods (available on the *Blood* Web site) describes additional details.

Retrovirus infection and BM transplantation

Murine *Mycn* complementary DNA was cloned into the retroviral vector pMXs-IG as described previously.[17] Mx1-Cre expression was induced by intraperitoneal injection of 7- to 8-week-old *Mx1-Cre*(+);*Fzr1*$^{f/f}$ mice (with *Mx1-Cre*(−);*Fzr1*$^{f/f}$ mice as controls) with polyinosinic-polycytidylic acid (pIpC; 25 μg per gram bodyweight) (Sigma-Aldrich, St. Louis, MO) on 5 successive days. Both groups of mice were selected from among the same littermates for each experiment. The mice were injected intraperitoneally with 150 mg/kg 5-fluorouracil (Kyowa Hakko Kirin, Tokyo, Japan) at 4 weeks after the final pIpC injection, and bone marrow mononuclear cells (BM-MNCs) were isolated 2 days later with the use of Lympholyte-M (Cedarlane, Uden, The Netherlands). The cells were cultured for 2 days in α–minimum essential medium (Invitrogen, San Diego, CA) supplemented with 20% fetal bovine serum, 100 U/mL penicillin, 100 U/mL streptomycin, 55 mM 2-mercaptethanol, 100 ng/mL recombinant mouse stem cell factor (Peprotech, London, UK), and 50 ng/mL recombinant human interleukin-6 (Peprotech) before infection with a retrovirus encoding *Mycn* and *GFP* as described previously.[17] For generation of recombinant retrovirus, the corresponding retroviral vector was introduced into Platinum-E packaging cells[19] by transfection with the use of the Fugene HD reagent (Promega, Madison, WI) and incubation of the cells overnight at 37°C under 5% CO_2. The medium was then replaced, and cells were incubated for an additional 48 hours before collection of culture supernatants. The supernatants were filtered with the use of a 0.45-μm cellulose acetate filter (Iwaki, Tokyo, Japan) for isolation of the recombinant retrovirus. Retroviral infection of BM-MNCs was performed for 3 days in 35-mm dishes coated with RetroNectin (Takara Bio, Tokyo, Japan). The cells were then collected by exposure to cell dissociation buffer (Invitrogen) for transplantation into mice. Infected (green fluorescent protein [GFP]$^+$) cells (5×10^4) were injected IV into WT C57BL/6 mice that had been subjected to sublethal irradiation (4 Gy). For secondary and tertiary transplantation, BM-MNCs were harvested from moribund mice, and GFP$^+$ cells (5×10^4) were transferred to WT recipients as for the primary transplants. When moribund, 2 primary transplant mice were selected from each of the *Fzr1*-deficient group and the *Fzr1*-intact group for injection of BM-MNCs into secondary recipients. Survival times of these mice at primary transplantation were 94 and 96 days in *Fzr1*-deficient and 90 and 94 days in *Fzr1*-intact mice.

Gene expression profiling

Total RNA was extracted from sorted GFP$^+$ BM-MNCs using Trizol reagent (Invitrogen) and RNeasy Mini kits (QIAGEN Inc., Hilden, Germany) from GFP$^+$ BM-MNCs. Biotin-labeled aRNA probes were synthesized from total RNA and subjected to hybridization with the Mouse Genome 430 2.0 Array (Affymetrix, Santa Clara, CA). Raw intensity data were normalized and analyzed using R statistical programming language (version 2.12.1; http://www.r-project.org) and robust multiarray analysis.[20] Differentially expressed genes were identified using the Linear Models for Microarray Analysis Data program (http://www.bioconductor.org/packages/release/bioc/html/limma.html).[21] Gene set enrichment analysis (GSEA)[22] software version 2.0.7 with Molecular Signatures Database gene sets (version 3.0) was used to analyze genes ranked according to the *Fzr1*-deficient/*Fzr1*-intact transcript ratio. Gene sets with *P* values less than 0.05 plus false-discovery rates less than 0.25 were considered significant. The data from our microarray studies have been submitted to the Gene Expression Omnibus (accession number GSE69863; http://www.ncbi.nlm.nih.gov/geo/query/acc.cgi?token=ctqrmmswzrwdfot&acc=GSE69863).

RPPA

Patient specimens were acquired during diagnostic assessment and analyzed in accordance with regulations and protocols approved by the MD Anderson Investigational Review Board. Informed consent was obtained from all patients in accordance with the Declaration of Helsinki. Detailed methods and validation of proteomic profiling were described previously.[23] Peripheral blood (PB) and BM specimens were collected from 224 B-ALL patients (207 newly diagnosed and 17 relapsed) who were evaluated at The University of Texas MD Anderson Cancer Center. All samples remained on ice until processing (typically within 2 hours of collection). All protein preparations were made from fresh (not

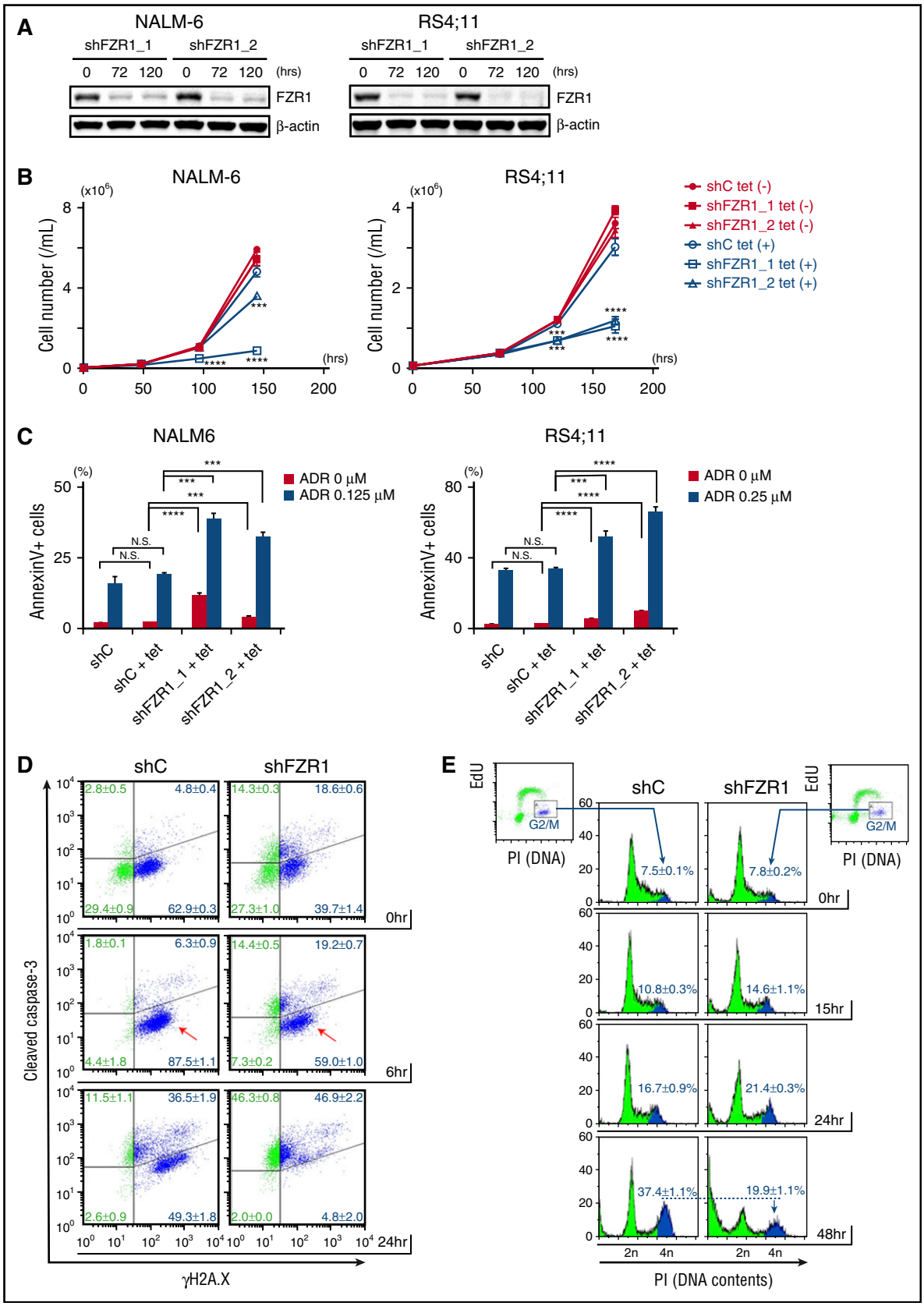

Figure 3. *FZR1* knockdown sensitizes human B-ALL cells to DNA damage–induced cell death and mitotic catastrophe. (A) Immunoblot of FZR1 in NALM-6 and RS4;11 cells transduced with lentivirus expressing tetracycline-inducible control (C) shRNA or shRNA specific to *FZR1* (shFZR1_1 and shFZR1_2) after 72-hour and 120-hour treatment with 1 μg/mL tetracycline. (B) Time-course cell proliferation assay of NALM-6 and RS4;11 cells with tetracycline-induced shC or shFZR1 treated with tetracycline (0.25 μg/mL for NALM-6 cells and 0.10 μg/mL for RS4;11). Trypan blue–negative cells were counted at described time points. *P* values were calculated by comparing with untreated controls. (C) Apoptosis analysis of NALM-6 and RS4;11 cells with tetracycline-induced shC or shFZR1 after treatment with tetracycline and doxorubicin. Cells were

cryopreserve), cells on the day of collection. Clinical details, including responses and outcomes, were collected for 172 of the patients with newly diagnosed disease (supplemental Table 1). Additional normal specimens were collected as controls, including $CD34^+$ BM cells (N = 16), $CD133^+$ BM cells (N = 5), and PB-MNCs (N = 9). Antibodies against FZR1 (LifeSpan BioSciences, Seattle, WA) and MYC (Cell Signaling Technology) were validated and used for RPPA analysis as described previously.[23] The level of FZR1 expression for all 224 B-ALL specimens as determined by RPPA analysis was compared with that of normal BM and PB specimens. RPPA data for the 172 clinically annotated specimens of newly diagnosed B-ALL were used for analysis of clinical outcomes based on levels of FZR1 and MYC. The threshold for high vs low expression was set as the maximum expression level in normal $CD34^+$ BM cells.

Results

Overexpression of *Mycn* in *Fzr1*-intact or *Fzr1*-deficient BM cells confers the B-ALL phenotype

To determine the role of FZR1 in MYC-induced leukemogenesis, we examined the effect of *Fzr1* loss on the development of B-ALL in mice. *Fzr1*-intact ($Fzr1^{f/f}$) or *Fzr1*-deficient ($Fzr1^{\Delta/\Delta}$) BM-MNCs of conditional *Fzr1* GT mice were infected with a retrovirus harboring *Mycn* as well as an internal ribosome entry site and a GFP gene construct, and the infected cells were then injected into sublethally irradiated WT mice (Figure 1A). Diagnosis of B-ALL was determined by detection of $GFP^+/B220^+/IgM^-/CD3^-/Gr1^-/Mac1^-$ cells in PB and BM or in lymph nodes (LNs) for animals with lymphadenopathy. Both groups of recipient mice manifested a similar B-ALL phenotype with similar incidence rates (70% in the *Fzr1*-intact group vs 80% in the *Fzr1*-deficient group; $n = 20$ mice for each group, $P = .72$). GFP^+ cells were detected in PB 9 weeks after transplantation, and there was no significant difference in the percentage of such cells between the 2 groups (Figure 1B). Whereas all recipient mice manifested B-ALL in BM, 4 out of 7 mice in the *Fzr1*-intact group and 5 out of 7 mice in the *Fzr1*-deficient group had lymphadenopathy. There were no differences in leukemia cell morphology or immunophenotype (uniformly $B220^+/IgM^-/CD3^-/Gr1^-/Mac1^-$ uniform blast cells) between the recipients of *Fzr1*-intact or *Fzr1*-deficient cells (Figure 1C; supplemental Figure 1A). More than 95% of cells in all affected LNs were positive for Ki67 in both groups (Figure 1D), indicating that *Fzr1* loss did not affect the proportion of proliferating cells.

To confirm the GT for *Fzr1* in *Fzr1*-deficient B-ALL cells, we performed genomic polymerase chain reaction (PCR) analysis of sorted GFP^+ cells from BM or lymph nodes of both recipient groups (Figure 1E; supplemental Figure 1B). All of the examined *Fzr1*-deficient lesions were positive for the smaller recombined PCR products and negative for the larger ones derived from the *Fzr1* complementary DNA site, indicating that tumor cells indeed uniformly lack this site in the recipients of *Fzr1*-deficient BM-MNCs.

Increased survival time of mice with *Fzr1*-deficient B-ALL is associated with increased B-ALL cell death

Despite the similar pathological phenotypes of the 2 groups of recipient mice, the median survival time of the *Fzr1*-deficient group was significantly longer than that of the *Fzr1*-intact group (95 vs 78 days) (Figure 2A). We obtained similar results with recipients of BM cells from *Fzr1* heterozygous GT vs WT mice in the same B-ALL model (supplemental Figure 2A), demonstrating that longer survival of B-ALL mice is also achieved with *Fzr1* haploinsufficiency.[10] Given that the proportion of $Ki67^+$ cells did not differ between the *Fzr1*-intact and *Fzr1*-deficient groups (Figure 1D), we speculated that reduced viability of *Fzr1*-deficient B-ALL cells might be responsible for the survival advantage of mice harboring these cells. Consistent with this, affected LNs in the *Fzr1*-deficient group manifested a more prominent "starry-sky" histopathology (indicating focal areas of cell death) than those in the *Fzr1*-intact group (Figure 2B-C). We confirmed that most cells in the starry-sky regions were apoptotic (supplemental Figure 2B). The starry-sky pattern is a result of high tumor proliferation rate and subsequent apoptosis. It clinically assessed on the basis of Ki67 positivity and indicates progressive lymphoid malignancy. However, given the similar levels of Ki67 positivity in our 2 experimental groups of recipient mice (Figure 1D), we concluded that the lesions in the *Fzr1*-deficient animals reflect increased susceptibility to cell death, in addition to a high proliferation rate.

Fzr1 loss increases mitotic cell death due to DNA damage in B-ALL cells in vivo

To determine why *Fzr1*-deficient B-ALL cells are more prone to cell death than *Fzr1*-intact cells, we performed gene expression profiling for GFP^+ BM cells isolated from the 2 groups of recipients ($n = 3$ per group). GSEA revealed that 3 gene sets related to mitosis or the DNA damage response (DDR) were significantly enriched in the *Fzr1*-deficient cells (Table 1; supplemental Figure 3), suggesting greater activation of DDR at the G_2-M checkpoint with *Fzr1* deficiency. We therefore hypothesized that increased susceptibility to cell death in *Fzr1*-deficient B-ALL cells results from accumulation of DNA damage in G_2-M phase and that apparent activation of the G_2-M checkpoint gene signature reflects insufficient ability to overcome checkpoint dysfunction due to *Fzr1* loss.

To examine the relationship between mitosis or DNA damage and cell death, we stained B-ALL–affected LNs obtained from mice in the *Fzr1*-deficient and *Fzr1*-intact groups for phosphorylated histone H3 (pHH3) and histone γH2A.X. The number of $pHH3^+$ cells in the starry-sky lesions tended to be higher in the *Fzr1*-deficient group than in the *Fzr1*-intact group (Figure 2D-E), suggesting that *Fzr1* loss might increase the rate of mitotic cell death. Similarly, the number of $\gamma H2A.X^+$ cells in the areas of cell death was significantly higher in the *Fzr1*-deficient group (Figure 2F-G), indicating that loss of *Fzr1* impairs the ability of B-ALL cells to overcome cell death signaling triggered by DNA DSBs. These results thus suggested that a normal G2-M checkpoint via intact *Fzr1* protects B-ALL cells from DNA DSBs by repairing DNA damage properly in vivo.

Conditional knockdown of *FZR1* in human B-ALL cell lines has antileukemia effects and sensitizes cells to DNA damage–induced apoptosis and mitotic catastrophe

To determine the role of FZR1 in leukemia progression and in DNA damage–induced cell death, we generated human B-ALL cell

Figure 3 (continued) treated with tetracycline (0.125 μg/mL for NALM-6 and 0.10 μg/mL for RS4;11) for 5 days and then treated with doxorubicin (0.125 μM for NALM-6 and 0.25 μM for RS4;11) for 36 hours. Annexin V–positive cells were counted by flow cytometry. (D) Costaining of γH2A.X and cleaved caspase-3 in NALM-6 cells with tetracycline-inducible shC or shFZR1 (shFZR1_1). Cells were treated with 0.125 μg/mL tetracycline for 5 days and then treated with 0.5 μM doxorubicin. (E) Flow cytometric analysis of 5-ethynyl-2′-deoxyuridine (EdU) incorporation combined with DNA content analysis with propidium iodide (PI) staining in NALM-6 cells with tetracycline-inducible shC or shFZR1 (shFZR1_1). Cells were treated with 0.125 μg/mL tetracycline for 5 days and then treated with 0.125 μM doxorubicin. Graphs in panels D and E are representative examples from 3 experiments. Except for panel A, results are expressed as mean ± SD (n = 3). $^*P < .05$, $^{**}P < .01$, $^{***}P < .001$, $^{****}P < .0001$.

lines with inducible knockdown of FZR1 using a tetracycline-inducible short hairpin RNA (shRNA) system. Among 7 B-ALL cell lines, we chose NALM-6, RS4;11, and Tanoue cells, which had the highest expression of both FZR1 and MYC proteins (supplemental Figure 4A). We transfected them with lentivirus carrying tetracycline-inducible shRNAs targeting *FZR1* (sh*FZR1*) or scramble control. Decreased FZR1 (75% to 90% reduction in protein expression) was confirmed by immunoblotting analysis (Figure 3A; supplemental Figure 4B). FZR1 knockdown showed antiproliferative effects with minimally induced apoptosis (Figure 3B-C; supplemental Figure 4C). This was consistent with our findings in vivo that mice bearing Fzr1-deficient B-ALL, and no additional perturbations, had slower progression and increased apoptosis as evidenced by enlarged starry-sky LN patterns (Figure 2A-B). Next, NALM-6 and RS4;11 cells with *FZR1* knockdown were treated with doxorubicin, a DNA damage inducer and a key drug in chemotherapy for B-ALL patients. We found that *FZR1* knockdown sensitized cells to doxorubicin-induced apoptosis (Figure 3C). We costained γH2A.X and cleaved caspase-3 and found that γH2A.X became positive in >90% of cells in both *FZR1* knockdown and *FZR1*-intact NALM-6 cells by 6 hours of doxorubicin treatment without a concomitant increase in cleaved caspase-3 (Figure 3D). Of note, γH2A.X was positive in 50% to 60% of NALM6 cells before doxorubicin treatment, consistent with the fact that cells in S phase are detected as positive for γH2A.X from DNA DSBs during DNA replication.[24] Cleaved caspase-3 was increased later by 24 hours of doxorubicin treatment (Figure 3D), demonstrating that the increased positivity of γH2A.X by 6 hours was not due to DNA fragments induced by an apoptotic process. The results demonstrated that *FZR1* knockdown did not affect the extent of doxorubicin-induced DNA damage but instead increased cell susceptibility to DNA damage–induced apoptosis. We further analyzed 5-ethynyl-2′-deoxyuridine incorporation combined with DNA contents analysis by propidium iodide staining in NALM-6 cells with *FZR1* knockdown. Accumulation of cells in G2-M phase, as normally induced by doxorubicin-induced DNA damage, was significantly reduced by *FZR1* knockdown (the percentage of cells in G2-M phase was 19.9% ± 1.1% in *FZR1* knockdown vs 37.4% ± 1.1% in *FZR1* intact cells; $P < .0001$) with increased cells noted in sub-G1 phase (Figure 3E; supplemental Figure 4D). This strongly suggested that mitotic catastrophe is involved in increased apoptosis, possibly due to G2-M checkpoint dysfunction caused by FZR1 knockdown. Reduction of cells in G1 phase was also observed, suggesting that FZR1 depletion may also promote DNA damage-induced apoptosis in G1 phase.

Low FZR1 expression is associated with a better clinical outcome in newly diagnosed, but not relapsed, B-ALL patients

To examine the clinical relevance of FZR1 expression in human B-ALL, we determined FZR1 abundance at the protein level with RPPA analysis of B-ALL cells derived from 224 patients. The level of FZR1 expression in specimens of newly diagnosed B-ALL was significantly higher than that in normal $CD34^+$ BM cells ($P = 6.02 \times$ e-9; supplemental Figure 5), ranging from the same level as that in normal $CD34^+$ cells (48.3%) to levels that were statistically significantly higher than the normal $CD34^+$ controls (51.7%). Given that B-ALL in our mouse model is induced by MYC overexpression, among the 172 clinically annotated specimens, we focused on 81 expressing high levels of MYC by RPPA relative to normal $CD34^+$ cells. The expression level of FZR1 was significantly lower in B-ALL from patients who achieved complete remission compared with those who did not achieve remission (Figure 4A), consistent with the increased susceptibility to cell death of murine *Fzr1*-deficient B-ALL cells. We next divided these 81 patients into 2 groups based on high vs low FZR1 expression. Remission duration was significantly increased for patients with a low level of FZR1 expression (Figure 4B). A proportional hazard (Cox) regression model was used to identify factors that are independent predictors of remission duration. Starting with 8 factors that were determined to be significant predictors in univariate analysis, a stepwise analysis was performed until only significant ($P < .05$) variables remained. The final model contained 5 variables: percent BM blasts, white blood cell count, CD10 positivity, *IKZF1* deletion, and FZR1 protein expression (Table 2). In addition, rate of relapse in patients with low FZR1 expression was significantly decreased compared with those with high FZR1 expression (39.5% vs 67.7%, $P = .019$). Despite the longer remission duration and lower relapse rate of patients with a low level of FZR1 expression, no significant difference in overall survival was apparent; however, the former patients showed a tendency toward longer survival (Figure 4C). We next selected patients who relapsed after complete remission from among the 172 clinically annotated patients with newly diagnosed B-ALL (n = 68). The survival time after relapse for these patients was short irrespective of FZR1 and MYC expression at initial diagnosis (Figure 4D), indicating that the clinical benefit associated with lower FZR1 expression may be transient and no longer apparent after relapse.

Serial transplantation of *Fzr1*-deficient B-ALL cells gives rise to progressive and resistant disease

To determine long-term in vivo outcomes of *Fzr1* deficiency in B-ALL, we performed secondary and tertiary transplantation of *Fzr1*-intact and *Fzr1*-deficient B-ALL cells in mice. Remarkably, the survival of comparison groups was the opposite of that predicted based on primary transplantation, where the *Fzr1*-deficient group had significantly shorter survival time than the *Fzr1*-intact group for both secondary and tertiary transplantation (Figure 5A). This finding suggested that increased susceptibility to cell death, thought to account for increased survival of mice undergoing primary transplant with *Fzr1*-deficient B-ALL cells, was less a factor in secondary or tertiary transplants. To assess the resistance of B-ALL cells to DNA damage, we irradiated mice 14 days after secondary transplantation of *Fzr1*-intact or *Fzr1*-deficient B-ALL cells. The increase in the number of GFP^+ cells in PB from the day of irradiation to 3 days afterward was significantly higher in the *Fzr1*-deficient group (Figure 5B). In addition, the survival time was significantly shorter in the irradiated *Fzr1*-deficient group (Figure 5C). Together, these results indicated that *Fzr1*-deficient B-ALL cells became more resistant to irradiation stress after serial transplantation.

Discussion

We have shown that loss of *Fzr1* results in two opposite, sequential effects on the survival of B-ALL cells in a mouse model. *Fzr1* deficiency initially confers sensitivity to genotoxic stress, however it also promotes expansion of increased robustness. The biphasic nature of *Fzr1* deficiency on leukemia cells over time is critical knowledge when considering therapies targeting FZR1 or affecting DDR.

Given that the antitumor effects on murine and human B-ALL cells were induced by *Fzr1* loss in the absence of any external perturbations (such as chemotherapy and irradiation), our findings support the notion

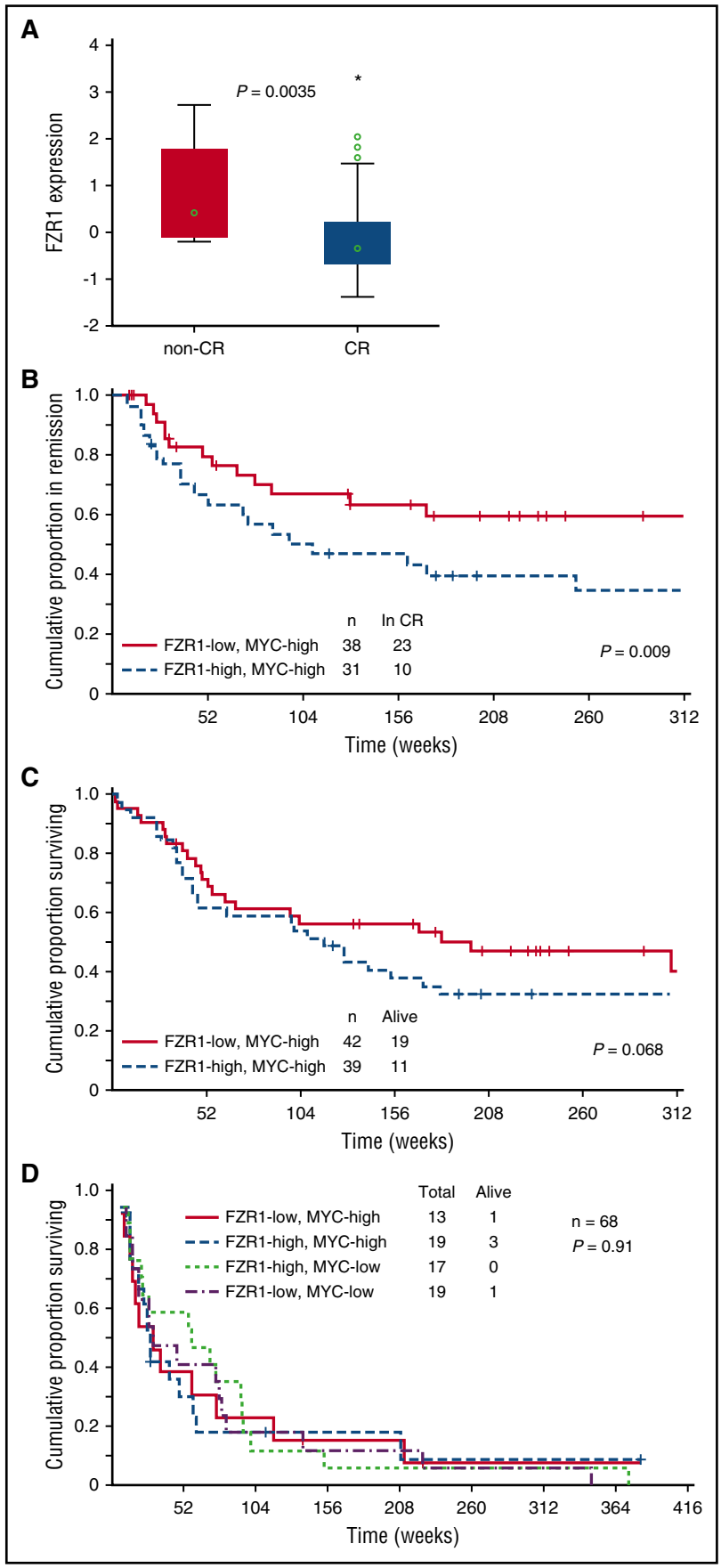

Figure 4. Relation of clinical characteristics to FZR1 and MYC expression levels in 172 B-ALL patients with clinically annotated specimens. (A) Comparison of FZR1 expression levels in B-ALL specimens obtained from patients with newly diagnosed disease who had high levels of MYC expression and either complete remission (CR; n = 69) or no remission (n = 12). The relation between FZR1 expression level and clinical response was evaluated with the Kruskal-Wallis test. (B) Remission duration stratified according to FZR1 expression level in the highly MYC-expressing (MYC-high) B-ALL specimens for the 69 patients in panel A who had complete remission. (C) Overall survival stratified according to FZR1 expression level in the MYC-high B-ALL specimens for the 81 patients in panel A. (D) Survival curves after relapse of B-ALL (68 of the 172 patients) stratified according to the levels of FZR1 and MYC expression in B-ALL specimens obtained at diagnosis.

Table 2. Multivariate analysis for remission duration

Variables	β	Standard error	β 95% lower	β 95% upper	*t*-value	Wald statistics	*P*	Risk ratio	Risk ratio 95% lower	Risk ratio 95% upper
BM blast	0.055839	0.024109	0.008587	0.103092	2.31616	5.36461	.020556	1.057428	1.008624	1.10859
WBC	0.008343	0.002316	0.003803	0.012883	3.60176	12.97268	.000317	1.008378	1.003810	1.01297
CD10	−0.019903	0.006291	−0.032234	−0.007572	−3.16351	10.00782	.001560	0.980294	0.968280	0.99246
IKZF1 del	2.271709	0.648224	1.001213	3.542205	3.50451	12.28160	.000458	9.695956	2.721581	34.54300
FZR1	0.956341	0.410727	0.151331	1.761351	2.32841	5.42149	.019897	2.602158	1.163381	5.82030

del, deletion; WBC, white blood count.

that FZR1 may be a candidate therapeutic target in B-ALL in context and that specific molecularly targeted therapy alone may be effective. Similarly, a therapeutic strategy for cancers based on targeting mitotic exit through inhibition of APC/C has been supported by several recent studies.[16,25,26] Furthermore, increased sensitivity to DNA damage–induced apoptosis by *FZR1* knockdown provides a rationale for targeting FZR1 in combination with standard genotoxic chemotherapy. Indeed, adult patients with a low level of FZR1 expression in B-ALL cells showed longer remission times and a lower risk of relapse than those exhibiting a high level of FZR1 expression. These results may be explained by the depth of complete remission as measured by the presence and quantity of minimal residual disease, which is an important predictor of remission duration and relapse for both childhood and adult ALL.[27-29] A low level of FZR1 expression in B-ALL cells may result in very deep complete remission and a lower relapse risk as a consequence of increased chemosensitivity of the cells.

Clonal heterogeneity and genetic variegation in tumorigenesis must be carefully taken into consideration in our mouse models, based on previous reports.[30-32] Even if leukemogenesis starts with clonal evolution from a preleukemic cell, secondary genetic changes can generate multiple subclones within a developed disease. Also, in our B-ALL mouse model, there was a latency period of several weeks (presumably a preleukemic stage) from primary transplantation to leukemia development, and it is likely that the secondary mutations and other genetic alterations were accumulated during this period. Therefore, we may not be able to assume that *Fzr1*-deficient and *Fzr1*-intact groups shared the exact same genetic subclones. Acknowledging this possible complexity in genetic heterogeneity, it is still reasonably possible that the overall difference in survival between 2 primary transplant groups was the direct result of the difference in *Fzr1* expression levels. This is because secondary genetic changes should have occurred stochastically in individual mice and provided the same extent of polyclonal conditions, and because we randomly selected 2 donor mice from individual groups at each transplantation to reduce the possibility of batch effects on genetic events. However, we cannot exclude the possibility that the difference in survival at primary transplant groups was actually due to the difference in secondary genetic changes that were unrelated to *Fzr1* deficiency. Additionally, the transition over time from a vulnerable state (primary transplant) to a robust state (secondary and tertiary transplant) of *Fzr1*-deficient B-ALL cells may be explained by a difference in secondary changes in the mechanistic balance between apoptosis signaling and cell survival.

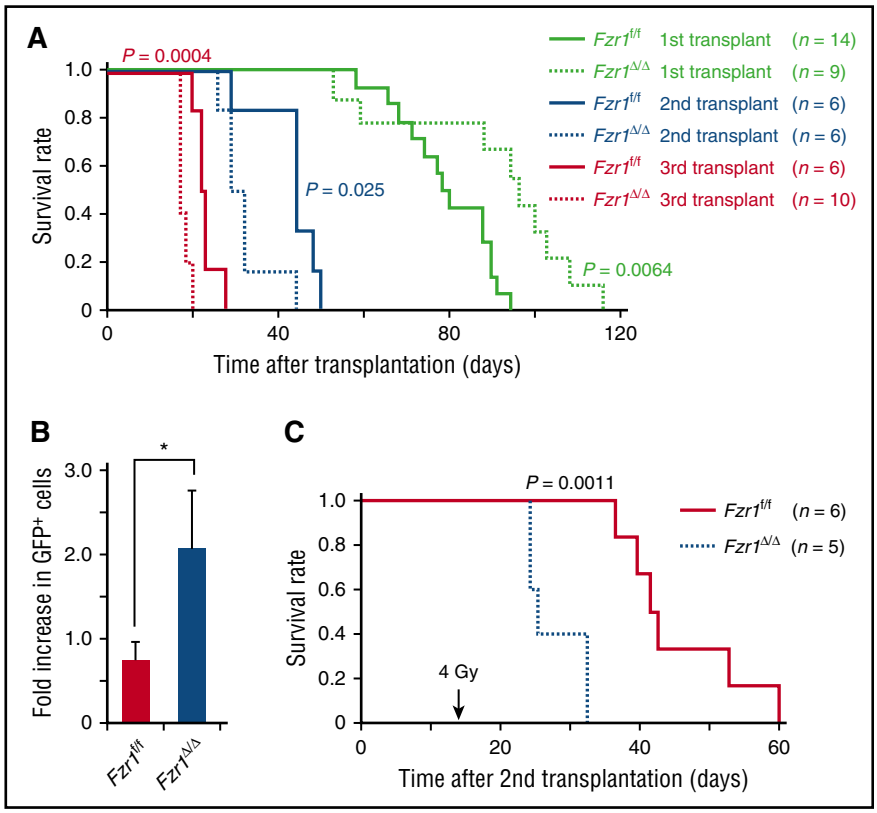

Figure 5. Serial transplantation of *Fzr1*-deficient B-ALL cells generates more progressive and resistant disease. (A) Survival curves for the indicated numbers of mice receiving primary, secondary, or tertiary transplants of *Fzr1*-intact or *Fzr1*-deficient B-ALL cells. *P* values for comparisons between the 2 types of B-ALL cells for each transplantation were determined with the log-rank test. The data for the primary transplant recipients are the same as those in Figure 2A. (B) Increase in the percentage of GFP$^+$ cells in PB between the day of and 3 days after irradiation for secondary transplant recipients that were irradiated 14 days after transplantation. Data are presented as mean ± SD (n = 3 mice per group); **P* = .0043. (C) Survival curves for the secondary transplant recipient mice as in (B). The *P* value for a comparison between the 2 groups was determined with the log-rank test (n = 6 mice for *Fzr1*-intact and 5 mice for *Fzr1*-deficient group).

The cell survival benefit may well be conferred by concomitant genetic instability directly caused by DDR dysfunction due to *Fzr1* loss. More specifically, *Fzr1* deficiency promotes aberrant G_2-M checkpoint signaling that, over the long-term, allows accumulation of gene mutations that result in clonal selection of cells resistant to DNA damage. Mutation analyses using next-generation sequencing and other clonality assays will be useful for further assessments on secondary genetic changes and clonal heterogeneity.

Robustness of tumor cells is defined as the ability to sustain cell survival even in the face of perturbations such as chemotherapy, irradiation, or cell stress as experienced in hypoxia or oxidative states. In addition to the need for comprehensive understanding of the mechanisms underlying robustness, identification of its vulnerabilities presents an opportunity for the development of new therapeutic approaches.[33] In the present study, we demonstrated the proof of concept that targeting of FZR1 as a key regulator of the DDR has the potential to undermine cancer cell robustness. However, persistent loss of FZR1 (and perhaps that of DDR regulators in general) ultimately confers a secondary state of robustness. While induction of synthetic lethality by targeting DDR remains a promising strategy for cancer therapy,[34-36] the transient vs tonic nature of inhibiting DDR regulatory molecules must now be carefully considered.

Acknowledgments

The authors thank K. Yamamura and K. Araki (Kumamoto University, Japan) for kindly providing *Fzr1* transgenic mice; M. Nakanishi, K. Nagata, S. Suzuki, I. Ishimatsu, Y. Ito, and S. Hayashi (Keio University) for technical assistance; O. Nagano, T. Shimizu, K. Kai, N. Onishi, and M. Tamada (Keio University) for technical advice; and K. Arai (Keio University, Japan) and D. Norwood (MD Anderson Cancer Center) for help with manuscript preparation.

This study was supported in part by a Japan Society for the Promotion of Science Postdoctoral Fellowship for Research Abroad Award (J.I.); the National Institutes of Health, National Cancer Institute (grants CA49639, CA100632, CA136411, and CA16672) and the Paul and Mary Haas Chair in Genetics (M.A.); the Leukemia & Lymphoma Society (grant 6089) (S.M.K.); and a grant from the Ministry of Education, Culture, Sports, Science, and Technology of Japan (H.S.). This study was also supported in part by research funding from Daiichi Sankyo Inc. and Eisai Co. Ltd. (H.S.).

Authorship

Contribution: J.I., E.S., S.K., and H.S conceived and designed the study; J.I., E.S., D.C., R.O.J., R.Z., Y.Q., and S.M.K. acquired data; J.I., E.S., K.M., K.K., C.B.B., S.Y.Y., S.M.K., and H.S. analyzed and interpreted data; J.I., E.S., C.B.B., S.M.K., and H.S. wrote, reviewed, or revised the manuscript; and N.H., S.O., and M.A. provided administrative, technical, or material support.

Conflict-of-interest disclosure: H.S. received research grants from Daiichi Sankyo Inc. and Eisai Co. Ltd. The remaining authors declare no competing financial interests.

Correspondence: Hideyuki Saya, Division of Gene Regulation, Institute for Advanced Medical Research, Keio University School of Medicine, Tokyo 160-8582, Japan; e-mail: hsaya@a5.keio.jp; and Steven M. Kornblau, Department of Leukemia, The University of Texas MD Anderson Cancer Center, Houston, TX 77030; e-mail: skornblau@mdanderson.org.

References

1. Peters JM. The anaphase promoting complex/cyclosome: a machine designed to destroy. *Nat Rev Mol Cell Biol*. 2006;7(9):644-656.
2. Sullivan M, Morgan DO. Finishing mitosis, one step at a time. *Nat Rev Mol Cell Biol*. 2007;8(11):894-903.
3. Pines J. Cubism and the cell cycle: the many faces of the APC/C. *Nat Rev Mol Cell Biol*. 2011;12(7):427-438.
4. Barford D. Structure, function and mechanism of the anaphase promoting complex (APC/C). *Q Rev Biophys*. 2011;44(2):153-190.
5. Pfleger CM, Kirschner MW. The KEN box: an APC recognition signal distinct from the D box targeted by Cdh1. *Genes Dev*. 2000;14(6):655-665.
6. Almeida A, Bolaños JP, Moreno S. Cdh1/Hct1-APC is essential for the survival of postmitotic neurons. *J Neurosci*. 2005;25(36):8115-8121.
7. Wirth KG, Ricci R, Giménez-Abián JF, et al. Loss of the anaphase-promoting complex in quiescent cells causes unscheduled hepatocyte proliferation. *Genes Dev*. 2004;18(1):88-98.
8. Skaar JR, Pagano M. Cdh1: a master G0/G1 regulator. *Nat Cell Biol*. 2008;10(7):755-757.
9. Engelbert D, Schnerch D, Baumgarten A, Wäsch R. The ubiquitin ligase APC(Cdh1) is required to maintain genome integrity in primary human cells. *Oncogene*. 2008;27(7):907-917.
10. García-Higuera I, Manchado E, Dubus P, et al. Genomic stability and tumour suppression by the APC/C cofactor Cdh1. *Nat Cell Biol*. 2008;10(7):802-811.
11. Sudo T, Ota Y, Kotani S, et al. Activation of Cdh1-dependent APC is required for G1 cell cycle arrest and DNA damage-induced G2 checkpoint in vertebrate cells. *EMBO J*. 2001;20(22):6499-6508.
12. Bassermann F, Frescas D, Guardavaccaro D, Busino L, Peschiaroli A, Pagano M. The Cdc14B-Cdh1-Plk1 axis controls the G2 DNA-damage-response checkpoint. *Cell*. 2008;134(2):256-267.
13. Ishizawa J, Kuninaka S, Sugihara E, et al. The cell cycle regulator Cdh1 controls the pool sizes of hematopoietic stem cells and mature lineage progenitors by protecting from genotoxic stress. *Cancer Sci*. 2011;102(5):967-974.
14. Naoe H, Araki K, Nagano O, et al. The anaphase-promoting complex/cyclosome activator Cdh1 modulates Rho GTPase by targeting p190 RhoGAP for degradation. *Mol Cell Biol*. 2010;30(16):3994-4005.
15. Lehman NL, Tibshirani R, Hsu JY, et al. Oncogenic regulators and substrates of the anaphase promoting complex/cyclosome are frequently overexpressed in malignant tumors. *Am J Pathol*. 2007;170(5):1793-1805.
16. Eguren M, Porlan E, Manchado E, et al. The APC/C cofactor Cdh1 prevents replicative stress and p53-dependent cell death in neural progenitors. *Nat Commun*. 2013;4:2880.
17. Sugihara E, Shimizu T, Kojima K, et al. Ink4a and Arf are crucial factors in the determination of the cell of origin and the therapeutic sensitivity of Myc-induced mouse lymphoid tumor. *Oncogene*. 2012;31(23):2849-2861.
18. Naoe H, Chiyoda T, Ishizawa J, Masuda K, Saya H, Kuninaka S. The APC/C activator Cdh1 regulates the G2/M transition during differentiation of placental trophoblast stem cells. *Biochem Biophys Res Commun*. 2013;430(2):757-762.
19. Morita S, Kojima T, Kitamura T. Plat-E: an efficient and stable system for transient packaging of retroviruses. *Gene Ther*. 2000;7(12):1063-1066.
20. Irizarry RA, Hobbs B, Collin F, et al. Exploration, normalization, and summaries of high density oligonucleotide array probe level data. *Biostatistics*. 2003;4(2):249-264.
21. Smyth GK. Linear models and empirical bayes methods for assessing differential expression in microarray experiments. *Stat Appl Genet Mol Biol*. 2004;3:Article3.
22. Subramanian A, Tamayo P, Mootha VK, et al. Gene set enrichment analysis: a knowledge-based approach for interpreting genome-wide expression profiles. *Proc Natl Acad Sci USA*. 2005;102(43):15545-15550.
23. Kornblau SM, Tibes R, Qiu YH, et al. Functional proteomic profiling of AML predicts response and survival. *Blood*. 2009;113(1):154-164.
24. Bonner WM, Redon CE, Dickey JS, et al. GammaH2AX and cancer. *Nat Rev Cancer*. 2008;8(12):957-967.
25. Zeng X, King RW. An APC/C inhibitor stabilizes cyclin B1 by prematurely terminating ubiquitination. *Nat Chem Biol*. 2012;8(4):383-392.
26. Zeng X, Sigoillot F, Gaur S, et al. Pharmacologic inhibition of the anaphase-promoting complex induces a spindle checkpoint-dependent mitotic arrest in the absence of spindle damage. *Cancer Cell*. 2010;18(4):382-395.

27. Cavé H, van der Werff ten Bosch J, Suciu S, et al; European Organization for Research and Treatment of Cancer–Childhood Leukemia Cooperative Group. Clinical significance of minimal residual disease in childhood acute lymphoblastic leukemia. European Organization for Research and Treatment of Cancer–Childhood Leukemia Cooperative Group. *N Engl J Med*. 1998;339(9):591-598.

28. Bassan R, Spinelli O, Oldani E, et al. Improved risk classification for risk-specific therapy based on the molecular study of minimal residual disease (MRD) in adult acute lymphoblastic leukemia (ALL). *Blood*. 2009;113(18):4153-4162.

29. Raff T, Gökbuget N, Lüschen S, et al; GMALL Study Group. Molecular relapse in adult standard-risk ALL patients detected by prospective MRD monitoring during and after maintenance treatment: data from the GMALL 06/99 and 07/03 trials. *Blood*. 2007;109(3):910-915.

30. Anderson K, Lutz C, van Delft FW, et al. Genetic variegation of clonal architecture and propagating cells in leukaemia. *Nature*. 2011;469(7330):356-361.

31. Oshima K, Khiabanian H, da Silva-Almeida AC, et al. Mutational landscape, clonal evolution patterns, and role of RAS mutations in relapsed acute lymphoblastic leukemia. *Proc Natl Acad Sci USA*. 2016;113(40):11306-11311.

32. Ma X, Edmonson M, Yergeau D, et al. Rise and fall of subclones from diagnosis to relapse in pediatric B-acute lymphoblastic leukaemia. *Nat Commun*. 2015;6:6604.

33. Kitano H. A robustness-based approach to systems-oriented drug design. *Nat Rev Drug Discov*. 2007;6(3):202-210.

34. Pearl LH, Schierz AC, Ward SE, Al-Lazikani B, Pearl FM. Therapeutic opportunities within the DNA damage response. *Nat Rev Cancer*. 2015;15(3):166-180.

35. Reaper PM, Griffiths MR, Long JM, et al. Selective killing of ATM- or p53-deficient cancer cells through inhibition of ATR. *Nat Chem Biol*. 2011;7(7):428-430.

36. Ruzankina Y, Schoppy DW, Asare A, Clark CE, Vonderheide RH, Brown EJ. Tissue regenerative delays and synthetic lethality in adult mice after combined deletion of Atr and Trp53. *Nat Genet*. 2009;41(10):1144-1149.